In situ study of the hot-working behavior of an advanced intermetallic multi-phase γ-TiAl based alloy

E. Schwaighofer[1], A. Stark[2], L. Lottermoser[2], R. Kirchhof[2], H. Clemens[1], N. Schell[2], and S. Mayer[1]

[1]*Department of Physical Metallurgy and Materials Testing, Montanuniversität Leoben, 8700 Leoben, Austria*

[2]*Institute of Materials Research, Helmholtz-Zentrum Geesthacht, 21502 Geesthacht, Germany*

Advanced intermetallic γ-TiAl based alloys, e.g. TNM alloys with a nominal composition of Ti-43.5Al-4Nb-1Mo-0.1B (in at.%), have a high potential to be used for turbine blades or turbo-charger wheels in the next generation of aircraft and automotive combustion engines [1–4]. The adjustment of balanced mechanical properties, i.e. high creep resistance combined with sufficient ductility at room temperature (RT), is strongly influenced by the hot-working behavior of the alloy.

In order to evaluate the hot-workability and processing parameters of a cast and hot-isostatically pressed (cast/HIP) TNM alloy, *in situ* deformation experiments were conducted with the high energy X-ray diffraction (HEXRD) setup of the HZG beamline HEMS (P07-EH3) at Petra III, DESY, Hamburg. The uniaxial compression tests were carried out under Ar-atmosphere in a quenching and deformation dilatometer DIL 805 A/D from Bähr Thermoanalyse GmbH, Germany, with a sample geometry of 10 mm in length and 5 mm in diameter. A scheme of the experimental procedure is shown in Fig. 1a. Therein, the sample was heated to 1300 °C above the γ-solvus temperature $T_{\gamma solv}$ with a heating rate of 400 K/min and held for 5 min. After holding the sample was continuously deformed under a linear cooling rate of ~2 K/s with a deformation rate of 0.005 s^{-1} to a total deformation of φ = -0.6 (equal to 60 % height reduction) followed by quenching with > 50 K/s to 600 °C. The diffraction patterns were recorded with a Perkin Elmer XRD 1622 flat panel detector with a frame rate of 2 Hz during the deformation cycle (E = 100 keV and beam size is 1·1 mm^2). The loading direction (LD) is parallel to the detector plane in order to eliminate textural effects on the evaluation of phase fractions as well as to study deformation-resolved texture evolution from a single detector image [5]. The evaluation of raw data respectively to azimuthal and 2Θ-integration as well as the generation of azimuthal-angle-time plots (AT-plots) was conducted by means of the software Fit2D [6,7]. TOPAS from Bruker AXS, USA, was used for Rietveld analysis. Texture analysis was performed with the program MAUD [8].

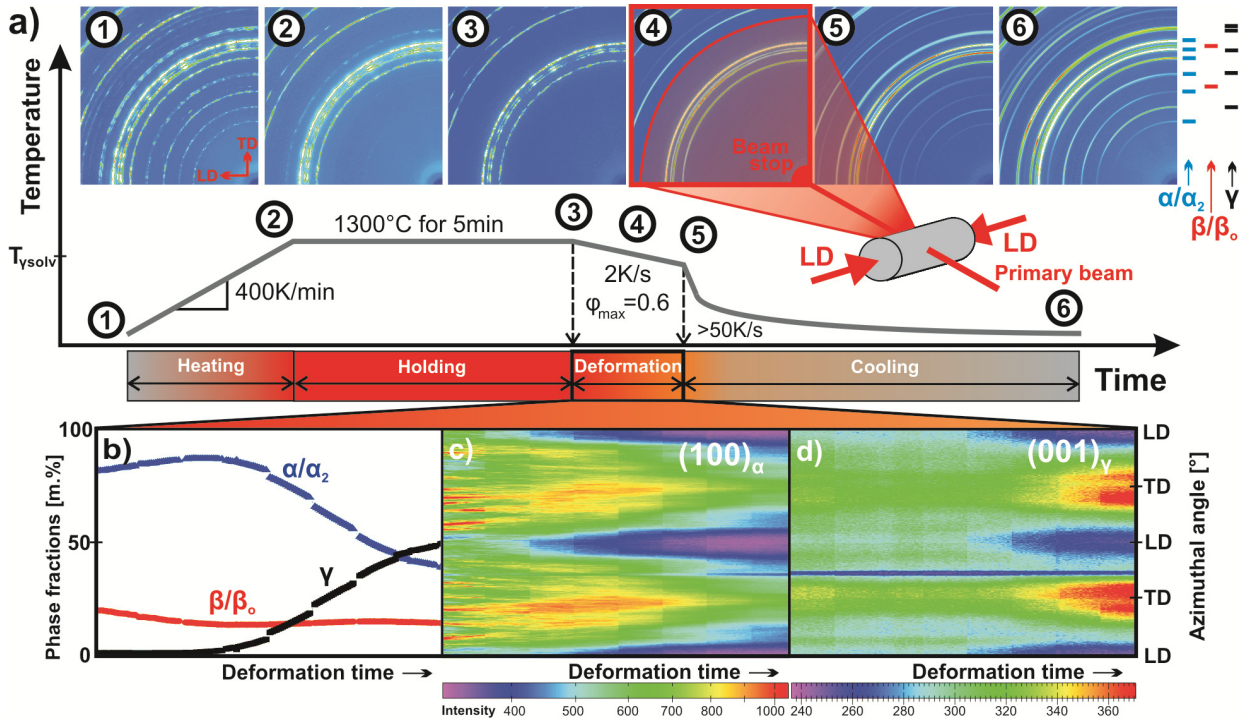

Figure 1: a) Time-temperature diagram and corresponding diffraction patterns of the investigated TNM alloy by means of a uniaxial compression experiment. b) Phase fraction evolution and AT-plots of c) $(100)_\alpha$- and d) $(001)_\gamma$-reflections during the deformation segment.

The time-temperature diagram in Fig. 1a was established to simulate near conventional forging conditions as reported in [9]. After heating to 1300 °C and isothermal holding (①-③) the intermetallic ordered phases α_2-Ti_3Al ($D0_{19}$-structure) and β_o-TiAl (B2-structure) disorder, whereby no grain growth of the disordered hcp α-phase takes place due to the presence of ~20 m.% disordered bcc β-phase. During the deformation sequence (③-⑤) the microstructure was refined. After deformation (⑤) and cooling to RT (⑥) a texture of the α_2- and γ-TiAl-phase ($L1_0$-structure) exists (see related detector images in Fig. 1a). Figure 1b shows the evolution of phase fractions during deformation. The β/β_o-phase remains nearly constant, whereas the γ-phase fraction increases at temperatures below $T_{\gamma solv}$ at the expense of α/α_2-phase. The texture evolution during deformation of the α/α_2- and γ-phase is shown in Figs. 1c and d. Thereby, the $(200)_{\alpha 2}$-reflection is treated as $(100)_{\alpha}$. Above $T_{\gamma solv}$, where no γ-phase exists, no significant texture occurs due to dynamic recrystallization (DRX) of the α-phase. Below $T_{\gamma solv}$ a texture occurs due to the formation of α/γ-colonies, which are more difficult to deform than a globular microstructure [10]. This implies a change in the deformation mode. Figure 2 compares the microstructure of the cast/HIP starting condition (Fig. 2a) with those after the deformation experiments. When the deformation is finished above $T_{\gamma solv}$, the microstructure consists predominantly of refined α_2-grains with weak texture due to DRX (Fig. 2b). The microstructure according to the experiment in Fig. 1a shows the formation of a tilted fiber texture of the α_2-phase (Fig. 2c). Additionally, DRX γ-grains are present. This refinement of coarse α-grains by DRX is a key factor to increase RT-ductility of γ-TiAl based alloys [10].

The experimental setup at HEMS beamline is a strong and powerful tool for the investigation of the hot-working behavior and provides important information, e.g. phase and textural evolution during deformation and subsequent cooling as well as the identification of DRX domains, which is required for the development of hot-working operations for the adjustment of balanced mechanical properties.

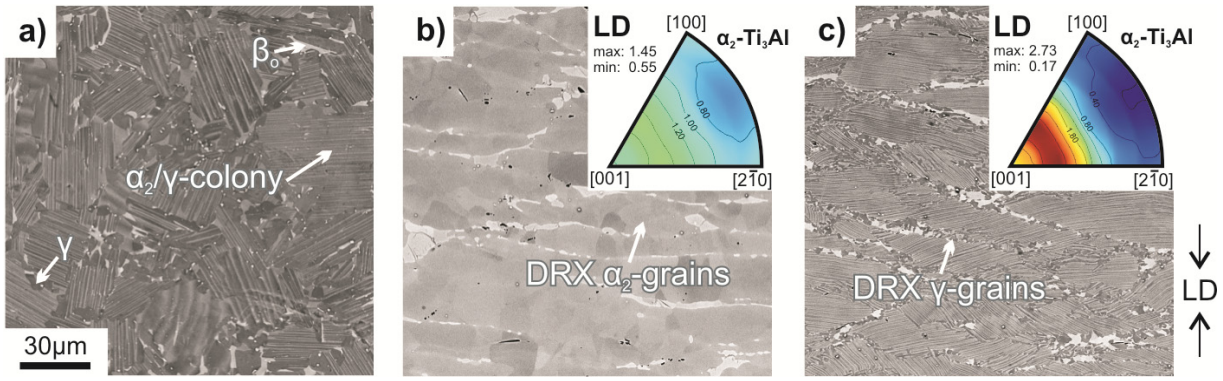

Figure 2: a) Cast/HIP starting microstructure corresponding to condition ① in Fig. 1a. b) Microstructure after deformation at T > $T_{\gamma solv}$. c) Microstructure after the deformation experiment in Fig. 1a (⑥). The inserts in b) and c) indicate the inverse pole figures of the α_2-Ti_3Al phase after deformation at RT (in LD).

References

[1] F. Appel, M. Oehring, and R. Wagner, Intermetallics **8**, 1283 (2000).
[2] T. Tetsui, K. Shindo, S. Kobayashi, and M. Takeyama, Scripta Materialia **47**, 399 (2002).
[3] Y. W. Kim, D. Morris, R. Yang, and C. Leyens, *Structural Aluminides for Elevated Temperature Applications* (TMS, Warrendale, 2008).
[4] H. Clemens and S. Mayer, Adv. Eng. Materials in press. DOI 10.1002/adem.201200231 (2013).
[5] A. Stark, E. Schwaighofer, S. Mayer, H. Clemens, T. Lippmann, L. Lottermoser, A. Schreyer, and F. Pyczak, MRS Proceedings **1516**, DOI 10.1557/opl.2012.1577 (2013).
[6] A. P. Hammersley, S. O. Svensson, M. Hanfland, A. N. Fitch, and D. Häusermann, High Pressure Research **14**, 235 (1996).
[7] K. D. Liss, T. Schmoelzer, K. Yan, M. Reid, M. Peel, R. Dippenaar, and H. Clemens, Journal of Applied Physics **106**, (2009).
[8] L. Lutterotti, M. Bortolotti, G. Ischia, I. Lonardelli, and H.-R. Wenk, Zeitschrift Für Kristallographie Supplements **2007**, 125 (2007).
[9] W. Wallgram, H. Clemens, and M. Schloffer, Patent Application Number 20110277891, (2011).
[10] Y.-W. Kim, Materials Science and Engineering A **192-193**, 519 (1995).